Characteristics of BF_2, Ga and In Implanted Si after FLA and RTA Annealing

Bo Wo[1)], Yusuke Matsunaga[1)], Siti Rahmah Binti Aid[1)], Satoru Matsumoto[1)], John Borland[2)], and Masayasu Tanjyo[3)]

1) Department of Electronics and Electrical Engineering, Keio University, 3-14-1, Hiyoshi, Kohoku-ku, Yokohama 223-8522, Japan
2) JOB Technologies, Aiea, Hawaii, USA
3) Nissin Ion Equipment Co., LTD, 575Kuze-Tonoshiro-cho, Minami-ku, Kyoto 601-8205, Japan

Abstract. The dopant diffusion, electrical activation, diode I-V characteristics and damage recovery of BF_2, Ga and In implanted Si after annealing have been investigated for samples with the peak concentration of $1.0x10^{19}cm^{-3}$ as p-type dopant atoms. Within this concentration, Ga implanted samples have the low sheet resistance and lowest leakage current in diode I-V with good crystallinity.

Keywords: P-type dopants in Si, electrical activation, leakage current, damage recovery.
PACS: 61.72.uf, 85.30.kk, 66.30.-h

INTRODUCTION

Ion implantation has been used widely to introduce dopants in MOSFET such as source/drain, extension, halo, well formation and channel doping. For p-type dopants, boron (B) has been exclusively used due to its high solid solubility.

It has been reported that the reverse short channel effect is observed in MOSFET's with boron channel and it is suggested that there is a possibility of boron pileup in the channel region at the edge of the source and drain regions due to the transient enhanced diffusion of boron during annealing [1].

Recently, indium (In) has been used for halo implantation for suppression of short channel effect [2]. However, there are few works on the characteristics of gallium (Ga) and In implanted Si after annealing.

In this work, we studied the dopant diffusion, electrical activation, diode characteristics and damage recovery of Ga and In implanted Si as well as BF_2 for p-type dopants in Si.

EXPERIMENTAL

The p-type dopant atoms of B, Ga and In have been implanted into n-type Si wafers with Nissin medium current implanter. BF_2 ion implantation was performed at the energy of 26 keV, Ga was implanted at 36 keV and In was implanted at 60 keV with doses of 1.5, 3.0 and $4.5x10^{13}cm^{-2}$, as summarized in Table 1. Implanted conditions were chosen to generate the same projected ranges and peak concentrations of as-implanted profiles for each sample. In addition to the above conditions, a combination of BF_2 (26 keV, $1.5x10^{13}cm^{-2}$) + In (60 keV, $3.0x10^{13}cm^{-2}$) and BF_2 (26 keV, $3.0x10^{13}cm^{-2}$) + In (60 keV, $3.0x10^{13}cm^{-2}$) were also performed.

The amorphous layer thickness of as-implanted samples was measured with ellipsometry. The values of the thickness for BF_2 and Ga implanted samples were varied from about 3 to 6 nm, increasing with the implanted doses. On the other hand, for In implanted samples, these values were to be 3 nm, 35 nm and 37 nm for doses of 1.5, 3.0 and $4.5x10_{13}cm^{-2}$, respectively. It is noted that amorphous layer thickness increased very rapidly above the dose of $3.0x10^{13}cm^{-2}$. In the case of the combination of BF_2 + In, amorphous layer thickness was about 34 nm, irrespective of BF_2 doses.

Annealing was performed using a 1200℃ Flash anneal followed by 900℃/10s RTA anneal.

Concentrations of dopant atoms were determined by secondary ion mass spectroscopy (SIMS). Sheet carrier concentration and sheet resistance were determined by Hall effect measurement. Mesa-type diodes were fabricated after annealing and their current (I) – voltage (V) characteristics were measured by HP semiconductor parameter analyzer.

The crystallinity near the junction of samples after annealing was analyzed by transmission electron microscope (TEM).

TABLE 1. Ion implantation conditions.

Dopant	Energy [keV]	Dose [10^{13}cm^{-2}]
BF_2	26	1.5, 3.0, 4.5
Ga	36	1.5, 3.0, 4.5
In	60	1.5, 3.0, 4.5

RESULTS

Dopant Profiles Before and After Annealing

Figure 1 shows the as-implanted profiles of BF_2, Ga and In for a dose of $3.0x10^{13}cm^{-2}$, which were obtained by TRIM simulation [3]. Although the Ga profile near the surface is steeper than that of BF_2, the peak concentration and projected range for BF_2 and Ga are almost the same, while In was implanted slightly deeper than those of BF_2 and Ga.

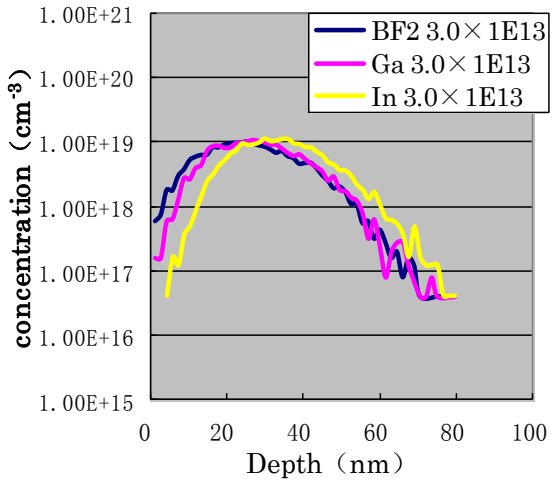

FIGURE 1. As-implanted profiles obtained by TRIM simulation

SIMS profiles after the Flash + RTA annealing are shown in Fig. 2. Each dopant atom diffuse in different ways. BF_2 and Ga profiles indicate pile-up at the surface, while In profile drops at the surface and has a significant peak at the depth of about 20 nm, which is shallower than the simulated projected range in Fig. 1. Ga diffuses deeper than BF_2 and In due to the higher diffusion coefficient of Ga at 1200℃[4].

Figure 3 shows the B concentration profiles for samples of $BF_2/3.0x10^{13}$ cm^{-2} and $In/3.0x10^{13}$ cm^{-2} + $BF_2/ 3.0x10^{13}$ cm^{-2}. Interesting point is that B diffusion is suppressed with the addition of In implantation. Since B is known to diffuse via self-interstitialcy mechanism, it suggests that the concentrations of Si

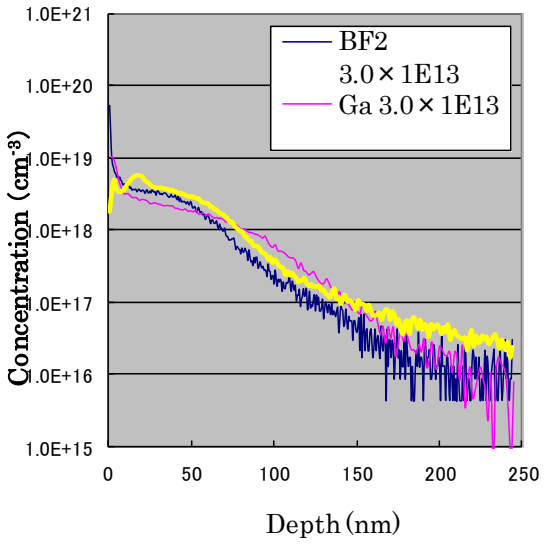

FIGURE 2. SIMS profiles after annealing

self-interstitials decrease with the presence of In. This result also indicates that In can be used as the pre-amorphization implantation for the formation of B shallow junction. Regarding In concentration profiles for samples of In/ $3.0x10^{13}$ cm^{-2} and $In/3.0x10^{13}$ cm^{-2} + $BF_2/ 3.0x10^{13}$ cm^{-2}, there was little difference in SIMS profiles.

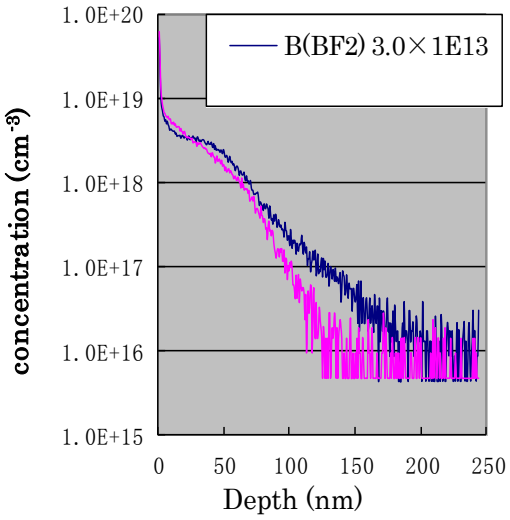

FIGURE 3. SIMS profiles of BF_2 and In + BF_2

Sheet Carrier Concentration and Sheet Resistance vs. Implanted Dose

Figure 4 shows the sheet carrier concentration as a function of implanted dose for BF_2, Ga and In, respectively. Sheet Hall coefficient *Rs* was determined by measuring the voltage change normal to the current path under a magnetic field perpendicular to the sample [5]. Then, sheet carrier concentration *Ns* was given by $Ns=r/eRs$, where *r* is the Hall factor and *e* is the electron charge. For a dose of $3.0x10^{13}cm^{-2}$, *Ns* of Ga is about 2/3 of BF_2 and *Ns* of In is about 1/8 of BF_2 as shown in Fig. 4. *Ns* is the number of carriers per cm^2, indicating an index of electrical activation. It is found that electrical activation of In implanted samples is very low as compared with that of BF_2.This is mainly due to the low solid solubility of In in Si. Although the accurate solid solubility of In at 1200℃ is obscure, its value seems to be around $1.0x10^{18}cm^{-3}$. Therefore, most of implanted In above this value in Fig. 3 may be inactive.

On the other hand, solid solubility of Ga at 1200℃ is $4x10^{19}cm^{-3}$, and that of B is $6x10^{20}cm^{-3}$ [4]. Since the peak concentration is about $1.0x10^{19}cm^{-3}$ as shown in Fig. 1, most implanted B and Ga are electrically activated in this experiment. The difference in sheet carrier concentration between BF_2 and Ga may be the difference in profiles at the depth from about 10 nm to 50 nm for respective dopants in Fig. 2.

The data of sheet carrier concentration of In + BF_2, which are not included in Fig. 4 are almost the same of those of BF_2. That is, electrically activated B atoms are contributed to the sheet carrier concentration as expected.

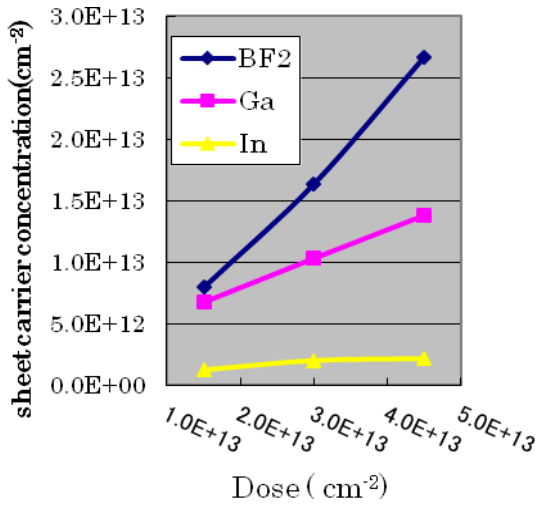

Figure 4. Sheet carrier concentration as a function of implanted doses

Figure 5 shows the sheet resistance (Rs) of BF_2, Ga and In implanted samples as a function of the dose. High sheet resistance of In samples comes from the poor electrical activation as shown in Fig. 4. On the other hand, Rs values of Ga and BF_2 samples are almost the same for the respective doses. It might be expected from the results of Fig. 4 that Rs values of Ga are larger than those of BF_2. However, both Rs values are almost the same. This is considered as follows. Ga atoms diffuse deeper than B atoms from the depth of about 50 nm as shown in Fig. 2. At this deeper region, Ga has the larger concentrations than those of BF_2 and it contributes to the reduction of Rs. Further detailed analysis is needed to approve this speculation.

Rs values of of In + BF_2 are almost the same as those of BF_2. Although there is some difference in profiles between BF_2 and In + BF_2, total active dopant quantities in Si substrate are considered to be almost the same in both cases.

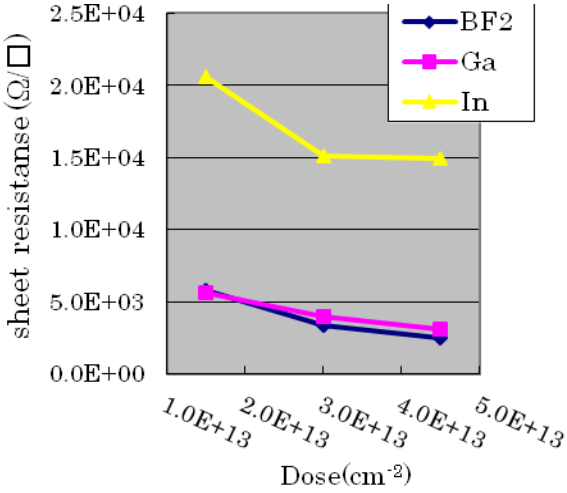

FIGURE 5. Sheet resistance (Rs) as a function of implanted doses

Diode I-V Characteristics

Figure 6 shows the diode I-V characteristics for BF_2, Ga and In implanted samples after annealing. As shown in Fig. 6, good forward I-V characteristics are obtained for respective dopants. Although a diode of BF_2 implanted sample has a large forward current, it also has a large reverse current, particularly, at small reverse voltages as compared with those of Ga and In implanted samples in the present experimental conditions. It is noted that a diode of Ga implanted sample has the lowest reverse current.

A diode of In + BF_2 sample has a smaller forward current than that of BF_2 and a larger reverse current than that of BF_2. That is, diode I-V characteristics of In + BF_2 sample are deteriorated as compared with that of BF_2 or In samples solely.

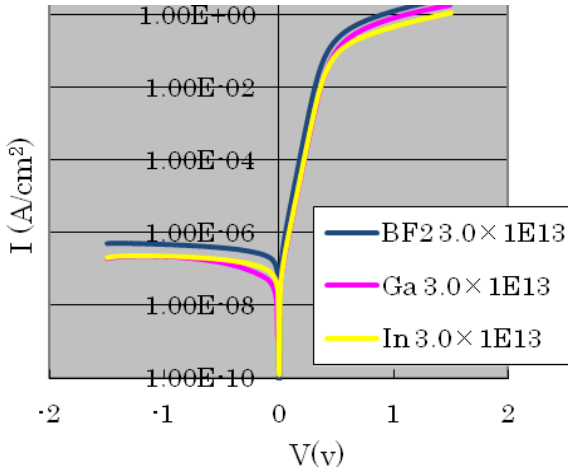

Figure 6. Diode I-V characteristics

Cross Sectional TEM Images

Figures 7 (a), (b), and (c) are the cross sectional TEM images of BF_2, Ga and In implanted samples, respectively. For BF_2 and Ga implanted samples, clear lattice images are observed from the surface to the bulk as shown in Fig. 7(a) and (b). Since the amorphous layer thickness of BF_2 and Ga implanted samples are 3 to 5 nm as described previously, damaged layer is recovered with good crystallinity.

On the other hand, for In implanted samples, some large defects are observed as shown in Fig. (c). Figure 7 (d) shows the TEM image of this defect with higher magnification. As shown, a distinct stacking fault is observed. It is pointed out that the position of these defects from the surface almost coincides with that of the significant peak in the profile in Fig. 2. It suggests that these defects are related with the agglomeration of inactive In atoms.

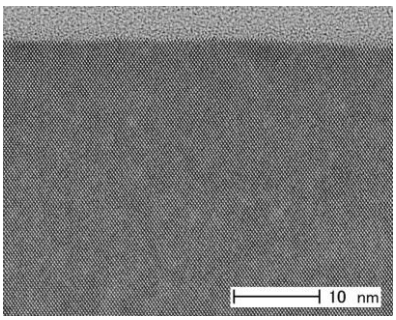

FIGURE 7(a). TEM image of BF_2 sample

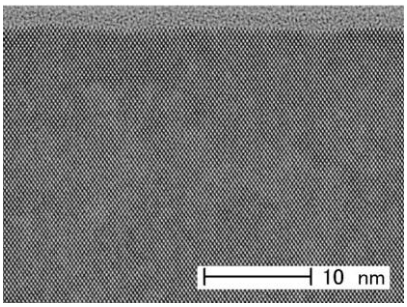

FIGURE 7(b). TEM image of Ga sample

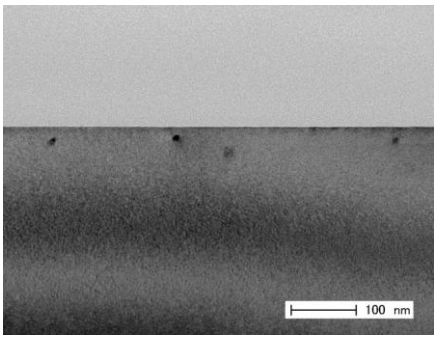

FIGURE 7(c). TEM image of In sample

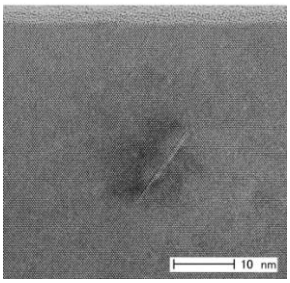

FIGURE 7(d). TEM image of In sample with higher magnification

REFERENCES

1. T. Mogami, The 11th International Workshop on Junction Technology 2011, Ext. Abs. p7
2. T. Sawada et al., Solid State Devices and Materials-2008, B-8-4, p.874
3. Homepage, http://www.strim.org/.
4. in Quick Reference Manual for Silicon Integrated Circuit Technology, edited by J. W. Beadle, J. C. C. Tsai and R. D. Plummer, New York, JOHN WILEY & SONS, 1985, pp 2-77.
5. J. W. Mayer, L. Eriksson and J. Davies, *Ion Implantation in Semiconductors*, New York, ACADEMIC PRESS, 1970, pp.186-188.